Abstract

An artificial nerve, in the broad sense, may be conceptualized as a physical and logical interface system that reestablishes the information traffic between the central nervous system and peripheral organs. Studies on artificial nerves targeting the autonomic nervous system are in progress to explore new treatment strategies for several cardiovascular diseases. First, we identified the rule for decoding native sympathetic nerve activity into heart rate using a transfer function analysis, and established a framework for a neurally regulated cardiac pacemaker. Second, we designed a bionic baroreflex system to restore the baroreflex buffering function using electrical stimulation of the celiac ganglion in a rat model of orthostatic hypotension. Third, based on the hypothesis that autonomic imbalance aggravates chronic heart failure, we implanted a neural interface into the right vagal nerve and demonstrated that intermittent vagal stimulation significantly improved the survival rate in rats with chronic heart failure following myocardial infarction. Although several practical problems need to be resolved, such as those relating to the development of electrodes feasible for long-term nerve activity recording, studies on the artificial neural interfaces with the autonomic nervous system have great possibilities in the field of cardiovascular treatment. We expect further development of the artificial neural interfaces as novel strategies to cope with cardiovascular diseases resistant to conventional therapeutics.

Key words: autonomic nervous system, arterial pressure, orthostatic hypotension, heart failure, transfer function

Introduction

Peripheral nerves are the pathways that convey information from peripheral organs to the central nervous system and commands from the central nervous system to peripheral organs. Damages to the peripheral nerves caused by injuries or diseases are disadvantageous to the living organs. In the narrow sense, an artificial nerve would indicate a replacement of the nerve fiber or nerve bundle with artificial materials capable of conducting nerve impulses. In the broad sense, the artificial nerve may be conceptualized as a physical and logical interface system that reestablishes the information traffic between the central nervous system and peripheral organs. Studies on artificial eyes and ears aim to restore sensory functions by building neural interfaces between artificial sensory devices and sensory nerves, the brainstem or the sensory cortex.[1-4] Studies on functional electrical stimulation aim to restore motor functions via electrical activation of lower motor neurons through stimulation of axons in peripheral nerves or within the spinal cord.[5] Functional electrical stimulation may also be applied directly to skeletal muscles.[6] In addition to these studies on artificial nerves relating to the sensory and motor systems, studies targeting the autonomic nervous system are in progress to explore new treatment strategies for cardiovascular diseases.

The heart has automaticity, which allows it to continue beating even in the absence of regulation by the autonomic nervous system. Loss of autonomic nervous regulation does not instantly terminate the circulation. In this sense, the significance of studies on the artificial nerves targeting the autonomic nervous system to treat cardiovascular diseases may be somewhat elusive compared with the studies related to the sensory and motor systems. However, the disruption of the autonomic nervous regulation critically affects activities of daily living. As an example, patients with severe orthostatic hypotension cannot maintain arterial pressure to keep consciousness during sitting or standing position and are forced to become bedridden. An artificial neural interface with the autonomic nervous system is expected to be an effective countermeasure to such diseased conditions. In this article, we will review our researches targeting the autonomic nervous system to treat cardiovascular diseases.

Neurally regulated cardiac pacemaker

A regulatory system of living organs, such as the autonomic nervous system, senses multiple physiological variables and controls the effector organs

accordingly. The first requirement in the development of an artificial neural interface system that can control effector organs is to decode native neural impulses quantitatively and interpret the commands from the central nervous system to the effector organs. In reference to the sympathetic heart rate control, although sympathetic activation is known to increase heart rate, a qualitative understanding of the input-output relationship is of little use in the development of a neurally regulated cardiac pacemaker. To examine the input-output relationship between these two variables, we measured left cardiac sympathetic nerve activity and heart rate in anesthetized rabbits.[7] The cervical vagal nerves were sectioned to avoid any vagal effects on heart rate. By imposing random pressure variations on the isolated carotid sinuses, we perturbed sympathetic nerve activity via the carotid sinus baroreflex. Plotting the instantaneous heart rate versus sympathetic nerve activity did not reveal any apparent correlations between the two signals (Fig. 1A). This is because the current heart rate is not determined solely by current sympathetic nerve activity but also influenced by the past history of sympathetic nerve activity.

In order to identify the dynamic input-output relationship between sympathetic nerve activity and heart rate, including the effect of past history, we employed a white noise analysis used in the engineering field (see Appendix for details). The transfer function from sympathetic nerve activity to heart rate approximated a low-pass filter (Fig. 1B). The response of heart rate became smaller and more delayed as the frequency of input perturbation increased. Berger *et al.* identified similar low-pass filter-like characteristics of sympathetic heart rate control using random electrical stimulation of the cardiac sympathetic nerve in anesthetized dogs.[8] When we calculated the impulse response via the inverse Fourier transform of the transfer function (see Appendix for details), the impulse response revealed a significant positive value for approximately 10 s. This result indicates that sympathetic nerve activity at any given time influences heart rate for approximately 10 s in rabbits (Fig. 1B). Once the impulse response is obtained, we can predict the output signal (heart rate) from the convolution integral between the input signal (sympathetic nerve activity) and the impulse response. Heart rate predicted from the measured sympathetic nerve activity demonstrated good agreement with the measured heart rate (Fig. 1C). Although several practical problems need to be resolved, accurate prediction of the instantaneous heart rate makes the framework using the transfer function extremely attractive as a principle for designing a neurally regulated cardiac

pacemaker.

Further comments on the transfer function analysis would help in-depth understanding. In the above-mentioned study,[7] we calculated the transfer function from left cardiac sympathetic nerve activity to heart rate. In reality, a branch of the left cardiac sympathetic nerve was sectioned and the nerve activity was recorded from the proximal end of the sectioned nerve. Therefore, the sympathetic nerve from which activity was recorded could not affect heart rate at the time of experiment. In addition, because the sinus node is predominantly innervated by the right cardiac sympathetic nerve, changes in heart rate are produced mainly by the right cardiac sympathetic nerve.[9] An implicit assumption of the study was that left cardiac sympathetic nerve activity could be the proxy of total sympathetic nerve activity that regulated heart rate. High coherence between left cardiac sympathetic nerve activity and heart rate is in support of this assumption (Fig. 1B). If the heart rate was regulated by a mechanism totally independent of left cardiac sympathetic nerve activity, the coherence function must have shown values close to zero. We verified our assumption by simultaneously recording left and right cardiac sympathetic nerve activities.[10] There was no apparent laterality of cardiac sympathetic nerve activities in response to dynamic carotid sinus baroreflex perturbation. The laterality observed in the sympathetic effects on the heart rate and ventricular contractility[9] may be mainly attributable to the different distributions of left and right cardiac sympathetic nerves within the heart.

Bionic baroreflex system

Multiple system atrophy (Shy-Drager syndrome) is caused by a disorder of the autonomic nervous system. Shy-Drager patients suffer from severe orthostatic hypotension because of the lack of a baroreflex buffering effect. Although counter measures to orthostatic hypotension are used such as administration of pressor agents and volume expansion, these treatments may induce supine hypertension. Ideal treatment would increase arterial pressure only when necessary, i.e., a position-dependent or more accurately a pressure-dependent pressor effect is required. In Shy-Drager patients, plasma noradrenaline levels are nearly normal in supine position and increase following tyramine administration, indicating that peripheral postganglionic sympathetic nerves are relatively spared but only weakly activated by postural changes.[11] If we can encode the information necessary for arterial pressure regulation and

deliver those signals to the postganglionic sympathetic system, orthostatic hypotension may be prevented using artificial sympathetic neural interventions.

Because a single nerve fiber discharges according to an all-or-nothing principle, it conveys information by frequency modulation. In contrast, multiple-fiber recording of a nerve bundle exhibits both frequency and amplitude modulations. This is because the amplitude of multiple-fiber recording is the weighted sum of concurrently discharging nerve impulses in the nerve bundle. Nerve fibers adjacent to the electrodes will contribute more to the amplitude generation. The ultimate goal of an artificial neural interface would be to create a respective interface with each nerve fiber in the bundle that could reproduce both the frequency and amplitude modulations. It is unrealistic at present, however, to establish such a complete interface, given the large number of nerve fibers and the small size of the interface.

An alternative strategy for neural interventions is to create a single neural interface to the whole nerve bundle and treat the system from nerve bundle stimulation to the effector response as a peripheral effector system. Using the electrical stimulation of the celiac ganglion, we explored the development of an artificial vasomotor center to restore normal arterial baroreflex function in rats with central baroreflex failure.[12,13] We first identified the dynamic characteristics of the carotid sinus baroreflex by imposing random pressure perturbations on the isolated carotid sinuses. The transfer function from baroreceptor pressure input to arterial pressure is defined as the native baroreflex function [$H_{Native}(f)$]. Next, we imposed random electrical stimulations on the celiac ganglion and quantified the transfer function from electrical stimulation to the arterial pressure response [$H_{Stim \rightarrow AP}(f)$]. Because the celiac ganglion governs a large abdominal vascular bed, electrical stimulation of the celiac ganglion effectively increased arterial pressure. The transfer function of the controller [$H_{Bionic}(f)$] was then determined in the frequency domain to fulfill the following equation (Fig. 2A, see Appendix for details).

$$H_{Bionic}(f)H_{Stim \rightarrow AP}(f) = H_{Native}(f)$$

In a typical experimental result (Fig. 2B), a head-up tilt did not decrease arterial pressure substantially in the rat with normal baroreflex. In contrast, the same head-up tilt caused significant hypotension in the rat with baroreflex failure. Activation of the bionic baroreflex system was able to restore the baroreflex buffering to a degree similar to that observed in the rat with normal baroreflex.

Note that native neural discharge of the celiac ganglion was not

recorded to develop the bionic baroreflex system,[12,13] whereas recording of the native cardiac sympathetic nerve activity was essential for the development of a neurally regulated cardiac pacemaker.[7] This distinction comes from the fact that the artificial vasomotor center was designed to control the peripheral effector system via electrical stimulation of the celiac ganglion to exert an arterial pressure response. A variety of interventions capable of changing arterial pressure can be treated as a peripheral effector of the bionic baroreflex system. We identified the transfer function from epidural spinal cord stimulation to the arterial pressure response and demonstrated that the bionic baroreflex system using epidural spinal cord stimulation could prevent orthostatic hypotension in anesthetized cats.[14] Yamasaki *et al.* applied the bionic baroreflex system using epidural spinal cord stimulation to prevent hypotension after sudden deflation of the thigh tourniquet in knee joint surgery.[15] Gotoh *et al.* demonstrated that an artificial neural interface with the vasomotor center (rostral ventrolateral medulla) provided rapid and precise control of arterial pressure in conscious rats.[16]

Bionic treatment against chronic heart failure

The autonomic nervous system plays an important role in maintaining the circulation under normal physiological conditions. Sympathetic activation and vagal withdrawal during exercise are beneficial to increase cardiac output in response to increased oxygen demand. Native autonomic regulation, however, does not always operate properly under diseased conditions. Heart failure develops when the heart can no longer provide adequate cardiac output to meet the oxygen demand. While sympathetic activation and vagal withdrawal help compensate for the reduced cardiac performance initially, sympathetic overactivity and vagal withdrawal eventually exacerbate the failing heart, resulting in sympathovagal imbalance and the vicious circle of chronic heart failure. Based on the pathological observation that sympathetic overactivity worsens heart failure, beta-adrenergic blockers and angiotensin converting enzyme inhibitors have been used as treatment. Although beta-blockers were long considered to be contra-indicated in heart failure, these drugs were ultimately demonstrated to improve outcome and are now established treatments.[17] Nevertheless, the therapeutic effect of sympathetic blockade is not always sufficient.

We hypothesized that vagal activation would also help terminate the vicious circle in chronic heart failure, and examined if vagal nerve stimulation

could treat chronic heart failure.[18] In halothane-anesthetized rats, the left coronary artery was ligated to produce myocardial infarction. One week later, a telemetry system to record arterial pressure and heart rate and a tele-stimulator system to stimulate the right vagal nerve were implanted under anesthetized conditions. Another week later (at 14 days after myocardial infarction), surviving rats were divided into vagal stimulation and control groups. In the vagal stimulation group, the right cervical vagal nerve was stimulated intermittently (10-s stimulation per minute) for 6 weeks. The intensity of vagal stimulation was adjusted to decrease heart rate by 20-30 beats/min. A 140-day follow-up revealed that vagal stimulation significantly increased the survival rate (Fig. 3). Although we did not directly treat the failing heart, the artificial neural interface to the vagal nerve ameliorated heart failure, thereby improved the survival rate.

The mechanisms by which vagal stimulation ameliorates chronic heart failure are not fully understood. Because vagal stimulation decreases heart rate, myocardial oxygen consumption is reduced. Vagal stimulation can also reduce ventricular contractility via the antagonism to the sympathetic effect,[19] which may also help reduce myocardial oxygen demand. Vagal stimulation shows anti-fibrillatory effect during ischemic insult in healed myocardial infarction in conscious dogs.[20] In acute myocardial ischemia, vagal stimulation reduces the accumulation of noradrenaline in the myocardial interstitium of the ischemic region.[21] Because catecholamines have cardiotoxicity,[22] reducing myocardial interstitial noradrenaline levels in the ischemic region may be cardioprotective. Vagal stimulation also reduces the protein levels of endogenous active matrix metalloproteinase-9 during ischemia-reperfusion injury,[23] which may contribute to the inhibition of ventricular remodeling. Because acetylcholine concentrations in the ischemic myocardium are increased via a local releasing mechanism that is independent of voltage dependent calcium channels,[24,25] vagal stimulation can only induce small additional increases in acetylcholine concentrations in the ischemic region.[21] Given the profound ameliorative effect of vagal stimulation in chronic heart failure,[18] the target of vagal effect may be the ischemic border zone, rather than the ischemic zone itself. Also, the vagal afferent pathway may modify the central nervous system to exert beneficial effects in chronic heart failure. Development of a new experimental method, such as that using reversible vagal blockade in conscious rats,[26] would help separate the afferent and efferent effects of vagal stimulation. Further studies are required to identify the mechanisms of cardioprotection by vagal stimulation.

Conclusion

In this review, we briefly summarized the studies of artificial neural interfaces targeting the autonomic nervous system with the goal of treating several cardiovascular diseases. In all of the studies discussed, creating a logical and physical interface with the autonomic nervous system is the key to effective cardiovascular treatment. In relation to the logical interface, we have demonstrated that the application of the white noise analysis was useful to decode and encode information for the autonomic nervous system. In relation to the physical interface, electrodes truly capable of long-term recording have not yet been realized. Although we examined the application of sieve-type nerve regeneration electrodes for stimulating and recording the autonomic nerves, further refinements are necessary for practical use. Studies of artificial neural interfaces with the autonomic nervous system are intriguing and have immense possibilities in the field of cardiovascular treatment. We expect further development of artificial neural interfaces as novel strategies to manage cardiovascular diseases that are resistant to conventional therapeutics.

Appendix A. Transfer function analysis

We resampled input-output data of sympathetic nerve activity and heart rate at 10 Hz, and segmented them into 8 sets of 50%-overlapping bins of 1024 points each. For each segment, a linear trend was subtracted and a Hanning window was applied. A fast Fourier transform was performed to obtain the frequency spectra of the input and output. Ensemble averages of input power spectra [$S_{XX}(f)$], output power spectra [$S_{YY}(f)$], and the cross spectra between the input and output [$S_{YX}(f)$] were then calculated. The transfer function was estimated from the following equation.[27]

$$H(f) = \frac{S_{YX}(f)}{S_{XX}(f)} \qquad \text{(A1)}$$

The coherence function between the input and output was calculated from the following equation.[27]

$$Coh(f) = \frac{|S_{YX}(f)|^2}{S_{XX}(f)S_{YY}(f)} \qquad \text{(A2)}$$

The coherence function ranges from zero to unity. Zero coherence indicates total independence between the input and output. Unity coherence indicates a perfect linear dependence of the output on the input.

Once the transfer function was identified, we could calculate the impulse response of the system [$h(\tau)$] via inverse Fourier transform of the transfer function. We then predicted the system response [$y(t)$] to an input signal [$x(t)$] from the convolution integral between $h(\tau)$ and $x(t)$ according to the following equation.

$$y(t) = \int_0^t h(\tau)x(t-\tau)d\tau \qquad \text{(A3)}$$

Although the above convolution integral predicts changes in the output signal in response to changes in the input signal, it cannot usually predict the direct current component or mean value of the output signal. In the case of the sympathetic heart rate control, heart rate does not become zero in the absence of sympathetic stimulation. In the prediction (Fig. 1C), we added the mean value of the measured heart rate to the output signal of the convolution integral to predict the absolute heart rate value.

Appendix B. Designing a bionic baroreflex system

The transfer function of the native baroreflex [$H_{Native}(f)$] determined the dynamic input-output relationship between baroreceptor pressure input [$P_{Input}(f)$] and arterial pressure [$AP(f)$] in the frequency domain.

$$AP(f) = H_{Native}(f)P_{Input}(f) \qquad \text{(B1)}$$

The transfer function from the stimulus command to arterial pressure [$H_{Stim\rightarrow AP}(f)$] determined the dynamic input-output relationship between the stimulus command [$C_{Stim}(f)$] and arterial pressure in the frequency domain.

$$AP(f) = H_{Stim\rightarrow AP}(f)C_{Stim}(f) \qquad \text{(B2)}$$

The transfer function of the bionic baroreflex [$H_{Bionic}(f)$] determined the dynamic input-output relationship between baroreceptor pressure input and stimulus command in the frequency domain.

$$C_{Stim}(f) = H_{Bionic}(f)P_{Input}(f) \qquad \text{(B3)}$$

From equations B2 and B3, the arterial pressure regulation by the bionic baroreflex can be described as follows.

$$AP(f) = H_{Stim\rightarrow AP}(f)H_{Bionic}(f)P_{Input}(f) \qquad \text{(B4)}$$

Comparison of equations B1 and B4 determined that the bionic baroreflex should fulfill the following equation to reproduce the native baroreflex function.

$$H_{Bionic}(f) = \frac{H_{Native}(f)}{H_{Stim \rightarrow AP}(f)} \quad \text{(B5)}$$

After determining the transfer function of the bionic baroreflex, we obtained the impulse response of the bionic baroreflex system [$h_{Bionic}(\tau)$] via inverse Fourier transform of the transfer function. We then calculated the stimulus command [$c_{Stim}(t)$] from the convolution integral between $h_{Bionic}(\tau)$ and baroreceptor pressure input [$p_{Input}(t)$] according to the following equation.

$$c_{Stim}(t) = \int_0^T h_{Bionic}(\tau) p_{Input}(t-\tau) d\tau \quad \text{(B6)}$$

In the above convolution integral, $p_{Input}(t)$ was treated as the change in arterial pressure from the arterial pressure value measured immediately before hypotensive intervention.

Acknowledgments

Supported in part by "Health and Labour Sciences Research Grant for Research on Advanced Medical Technology", "Health and Labour Sciences Research Grant for Research on Medical Devices for Analyzing, Supporting and Substituting the Function of Human Body", "Health and Labour Sciences Research Grant", from the Ministry of Health, Labour and Welfare of Japan.

References

1. Dowling J. Artificial human vision. Expert Rev Med Devices 2005;2:73-85
2. Walter P, Kisvárday ZF, Görtz M, Alteheld N, Rossler G, Stieglitz T, Eysel UT. Cortical activation via an implanted wireless retinal prosthesis. Invest Ophthalmol Vis Sci 2005;46(5):1780-1785
3. Papsin BC, Gordon KA. Cochlear implants for children with severe-to-profound hearing loss. N Engl J Med 2007;357:2380-2387
4. Lim HH, Lenarz T, Joseph G, Battmer RD, Samii A, Samii M, Patrick JF, Lenarz M. Electrical stimulation of the midbrain for hearing restoration: insight into the functional organization of the human central auditory system. J Neurosci 2007;27:13541-13551
5. Mushahwar VK, Jacobs PL, Normann RA, Triolo RJ, Kleitman N. New functional electrical stimulation approaches to standing and walking. J Neural Eng 2007;4(3):S181-S197
6. Sujith OK. Functional electrical stimulation in neurological disorders. Eur J Neurol. 2008; 15:437-444.
7. Ikeda Y, Sugimachi M, Yamasaki T, Kawaguchi O, Shishido T, Kawada T, Alexander J Jr, Sunagawa K. Explorations into development of a neurally regulated cardiac pacemaker. Am J Physiol 1995;269:H2141-H2146
8. Berger RD, Saul JP, Cohen RJ. Transfer function analysis of autonomic regulation. I. Canine atrial rate response. Am J Physiol 1989; 256:H142-H152
9. Miyano H, Nakayama Y, Shishido T, Inagaki M, Kawada T, Sato T, Miyashita H, Sugimachi M, Alexander J Jr, Sunagawa K. Dynamic sympathetic regulation of left ventricular contractility studied in the isolated canine heart. Am J Physiol 1998;275:H400-H408
10. Kawada T, Uemura K, Kashihara K, Jin Y, Li M, Zheng C, Sugimachi M, Sunagawa K. Uniformity in dynamic baroreflex regulation of left and right cardiac sympathetic nerve activities. Am J Physiol Regul Integr Comp Physiol 2003; 284:R1506-R1512
11. Parikh SM, Diedrich A, Biaggioni I, Robertson D. The nature of the autonomic dysfunction in multiple system atrophy. J Neurol Sci 2002; 200:1-10
12. Sato T, Kawada T, Shishido T, Sugimachi M, Alexander J Jr, Sunagawa K. Novel therapeutic strategy against central baroreflex failure: a bionic baroreflex system. Circulation 1999;100:299-304

13. Sato T, Kawada T, Sugimachi M, Sunagawa K. Bionic technology revitalizes native baroreflex function in rats with baroreflex failure. Circulation 2002;106:730-734
14. Yanagiya Y, Sato T, Kawada T, Inagaki M, Tatewaki T, Zheng C, Kamiya A, Takaki H, Sugimachi M, Sunagawa K. Bionic epidural stimulation restores arterial pressure regulation during orthostasis. J Appl Physiol 2004;97:984-990
15. Yamasaki F, Ushida T, Yokoyama T, Ando M, Yamashita K, Sato T. Artificial baroreflex: clinical application of a bionic baroreflex system. Circulation 2006;113:634-639
16. Gotoh TM, Tanaka K, Morita H. Controlling arterial blood pressure using a computer-brain interface. Neuroreport 2005;16:343-347
17. Mudd JO, Kass DA. Tackling heart failure in the twenty-first centry. Nature 2008;451:919-928
18. Li M, Zheng C, Sato T, Kawada T, Sugimachi M, Sunagawa K. Vagal nerve stimulation markedly improves long-term survival after chronic heart failure in rats. Circulation 2004;109:120-124
19. Nakayama Y, Miyano H, Shishido T, Inagaki M, Kawada T, Sugimachi M, Sunagawa K. Heart rate-independent vagal effect on end-systolic elastance of the canine left ventricle under various levels of sympathetic tone. Circulation. 2001;104:2277-2279
20. Vanoli E, De Ferrari GM, Stramba-Badiale M, Hull SS Jr, Foreman RD, Schwartz PJ. Vagal stimulation and prevention of sudden death in conscious dogs with a healed myocardial infarction. Circ Res 1991;68:1471-181
21. Kawada T, Yamazaki T, Akiyama T, Li M, Ariumi H, Mori H, Sunagawa K, Sugimachi M. Vagal stimulation suppresses ischemia-induced myocardial interstitial norepinephrine release. Life Sci. 2006;78:882-887
22. Rona G. Catecholamine cadiotoxicity. J Mol Cell Cardiol 1985;17:291-306.
23. Uemura K, Li M, Tsutsumi T, Yamazaki T, Kawada T, Kamiya A, Inagaki M, Sunagawa K, Sugimachi M. Efferent vagal nerve stimulation induces tissue inhibitor of metalloproteinase-1 in myocardial ischemia-reperfusion injury in rabbit. Am J Physiol Heart Circ Physiol 2007;293:H2254-H2261
24. Kawada T, Yamazaki T, Akiyama T, Sato T, Shishido T, Inagaki M, Takaki H, Sugimachi M, Sunagawa K. Differential acetylcholine release mechanisms in the ischemic and non-ischemic myocardium. J Mol Cell Cardiol 2000;32:405-414

25. Kawada T, Yamazaki T, Akiyama T, Uemura K, Kamiya A, Shishido T, Mori H, Sugimachi M. Effects of Ca^{2+} channel antagonists on nerve stimulation-induced and ischemia-induced myocardial interstitial acetylcholine release in cats. Am J Physiol Heart Circ Physiol 2006;291:H2187-H2191
26. Zheng C, Kawada T, Li M, Sato T, Sunagawa K, Sugimachi M. Reversible vagal blockade in conscious rats using a targeted delivery device. J Neurosci Methods 2006; 156:71-75
27. Marmarelis PZ, Marmarelis VZ. Analysis of Physiological Systems. The white noise method in system identification. New York: Plenum, 1978, p. 131-221.

Figure 1

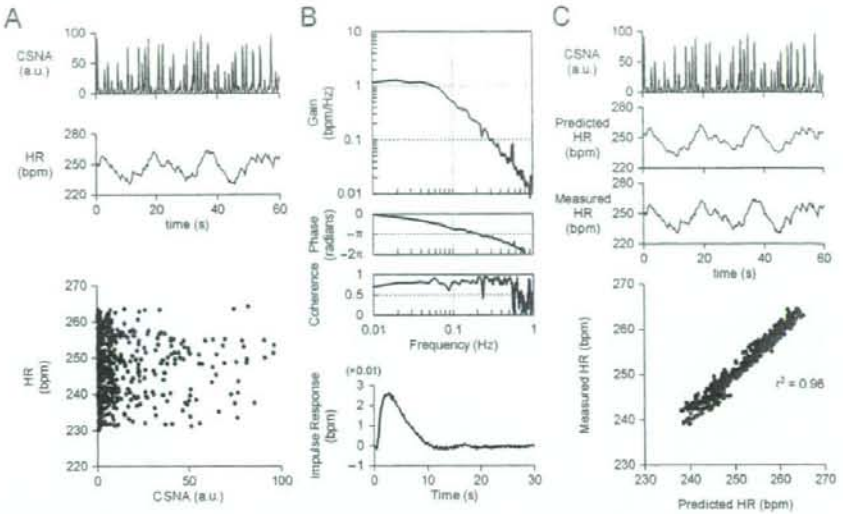

Decoding of sympathetic heart rate control (see Ref 7). A: Recordings of cardiac sympathetic nerve activity (CSNA) and heart rate (HR), which were plotted against each other. B: Transfer function from CSNA to HR and the corresponding impulse response. C: Prediction of HR from CSNA using the transfer function. A scatter plot of measured HR versus predicted HR displays the accuracy of this prediction.

Figure 2

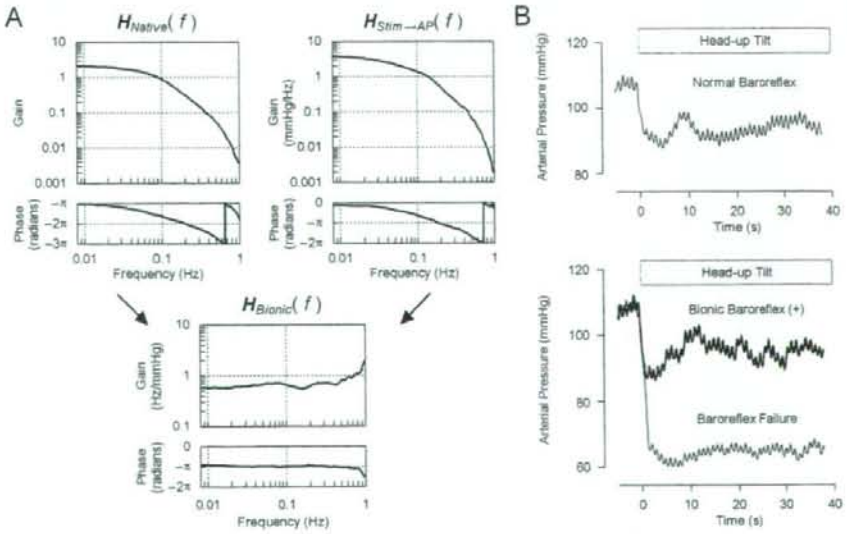

Arterial pressure regulation by the bionic baroreflex system (See Ref 13). A: Transfer function of the native baroreflex [$H_{Native}(f)$], transfer function from stimulation of the celiac ganglion to arterial pressure [$H_{Stim \rightarrow AP}(f)$], and transfer function of the bionic baroreflex [$H_{Bionic}(f)$]. B: Arterial pressure responses during head-up tilt in the rat with normal baroreflex (top) and in the rat with central baroreflex failure (bottom). Activation of the bionic baroreflex system restored the buffering effect against orthostatic hypotension.

Figure 3

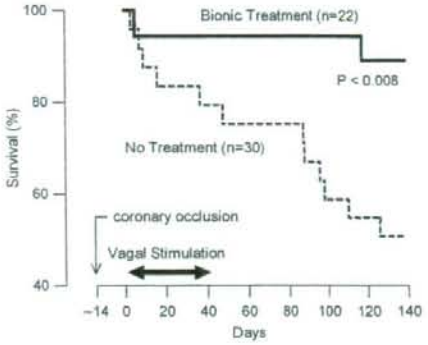

Survival of rats with chronic heart failure after myocardial infarction (see Ref 18). Vagal stimulation dramatically improved the survival rate.